

# High field magnetoresistance of nanocomposites (Co<sub>84</sub>Nb<sub>14</sub>Ta<sub>2</sub>)<sub>x</sub>(Al<sub>2</sub>O<sub>3</sub>)<sub>100-x</sub> near the percolation threshold

Mikhail Blinov<sup>1</sup>, Ivan Zakharchuk<sup>2</sup>, Erkki Lähderanta<sup>2</sup>, Alexander Sitnikov<sup>3</sup>, Igor Rodionov<sup>1</sup>, Valerii Prudnikov<sup>1</sup>, Vladimir Rylkov<sup>4,5</sup>, and Alexander Granovsky<sup>1,5</sup>

<sup>1</sup> Faculty of Physics, Lomonosov Moscow State University, 119991 Moscow, Russia

<sup>2</sup> Lappeenranta University of Technology, 53851 Lappeenranta, Finland

<sup>3</sup> Voronezh State Technical University, 394026 Voronezh, Russia

<sup>4</sup> National Research Centre “Kurchatov Institute”, 123182 Moscow, Russia

<sup>5</sup> Institute of Applied and Theoretical Electrodynamics RAS, 127412 Moscow, Russia

**Abstract.** We present results of experimental studies of magnetic properties, resistivity and magnetoresistance (MR) of (Co<sub>84</sub>Nb<sub>14</sub>Ta<sub>2</sub>)<sub>x</sub>(Al<sub>2</sub>O<sub>3</sub>)<sub>100-x</sub> films deposited onto a glass-ceramic substrate by the ion-beam sputtering, focusing on MR in high magnetic fields for compositions close to the percolation threshold ( $x=47-57$  at.%). The samples consist on Co-Nb-Ta metallic nanogranules size of 2-5 nm which are embedded into the non-stoichiometric Al-O matrix. Magnetization was measured by SQUID magnetometer at  $T=4.2-350$  K. MR was studied in the pulsed magnetic fields  $\mu_0H$  up to 20 T at  $T=70-300$  K in three geometries: magnetic field in plane parallel and perpendicular to current, magnetic field perpendicular to plane. The pulse duration was 11-12 ms. For the sample with  $x=57$  at.% the temperature dependence of conductivity follows the  $\ln T$  behavior that matches a strong tunnel coupling between nanogranules. With decreasing metal volume fraction  $\ln T$  behavior gradually changes to the  $T^{1/2}$  dependence at 47 at.%. For all samples MR is small (<1%) and negative. For  $x<57$  at.% it is slightly anisotropic at  $\mu_0H<1.0$  T and almost saturates with increasing magnetic field. There is an evidence of small positive contribution to MR at  $\mu_0H=20$ T. Accordingly to structural and magnetic data a large amount of metallic atoms are located between magnetic nanogranules that diminish the tunnel barrier height and make tunnel MR small and weakly dependent on temperature.

## 1 Introduction

Recent discovery of memristor effect in metal-insulator nanostructures, in particular in those based on non-stoichiometric oxides AlO<sub>z</sub> ( $z<1.5$ ) [1,2], triggered renewed interest to structural, magnetic and magnetotransport properties of magnetic nanocomposites [3,4]. In the case of (CoFeB)<sub>x</sub>(Al-O)<sub>1-x</sub> nanogranular thin films with metal content  $x=49-56$  at.% it was found a large number of Co, Fe and B atoms dispersed in Al-O matrix [3], logarithmic temperature dependence of conductivity [3, 4] and tunnel anomalous Hall effect [3]. These observations raised numerous questions on dominant transport mechanisms in nanocomposites. Particularly for mechanisms of magnetoresistance (MR), which may be due to tunneling, hopping, Lorentz force, spin-orbit interaction, weak localization and so on. The granular size about 2-5 nm and presence of isolated magnetic atoms in matrix requires for saturation of magnetization the use of high magnetic fields in MR measurements. In this paper we focus on MR in nanocomposites (Co<sub>84</sub>Nb<sub>14</sub>Ta<sub>2</sub>)<sub>x</sub>(Al-O)<sub>1-x</sub> in the pulsed magnetic fields  $\mu_0H$  up to 30 T.

## 2 Experiment

The nanocomposites (Co<sub>84</sub>Nb<sub>14</sub>Ta<sub>2</sub>)<sub>x</sub>(Al-O)<sub>1-x</sub> with  $x=47-57$  at.% were obtained by the ion-beam sputtering of targets, which consisted of a metal base of the Co<sub>84</sub>Nb<sub>14</sub>Ta<sub>2</sub> alloy with several Al<sub>2</sub>O<sub>3</sub> plates on its surface. Details of this method are presented in [3, 5]. The thickness of samples was about  $d=2.7\mu\text{m}$ .

The magnetization measurements were performed with a SQUID magnetometer (Cryogenic S700X) between 4.2 and 350 K at in-plane and out-of-plane magnetic fields  $\mu_0H$  up to 3 T.

The resistivity was measured with a standard dc method, and the pulsed magnetic field  $B$  up to 30 T was applied to measure the MR. The pulse duration was 11–12 ms. The magnetic field inhomogeneity did not exceed 3% within the size of the investigated area (5 mm<sup>2</sup>).

## 3 Results and discussion

### 3.1. Magnetization

The field and temperature dependencies of magnetization for studied samples (Fig.1) are quite

\* Corresponding author: gran60@mail.ru

typical for nanogranular thin films with compositions in the vicinity of percolation threshold [3]. The saturation field for in-plane geometry is less than that for out-of-plane case, increases gradually when  $x$  decreases from 57 to 47 at.%, and does not exceed 0.6-0.7 T. This behavior can be easily understood taking into account demagnetization effects. For example, the saturation field of 0.6-0.7 T is well coincided with the demagnetization of spherical Co particles. The data shown on Fig.1b indicates on superparamagnetic behavior. The temperature dependence of magnetization at 2.0 T (not shown) is similar to that reported in Ref. [3] (see Fig. 8c), namely, magnetization strongly increases at  $T < 25$  K due to presence of a large amount of metallic atoms located between magnetic nanogranules and is almost constant at  $T = 100-300$  K.

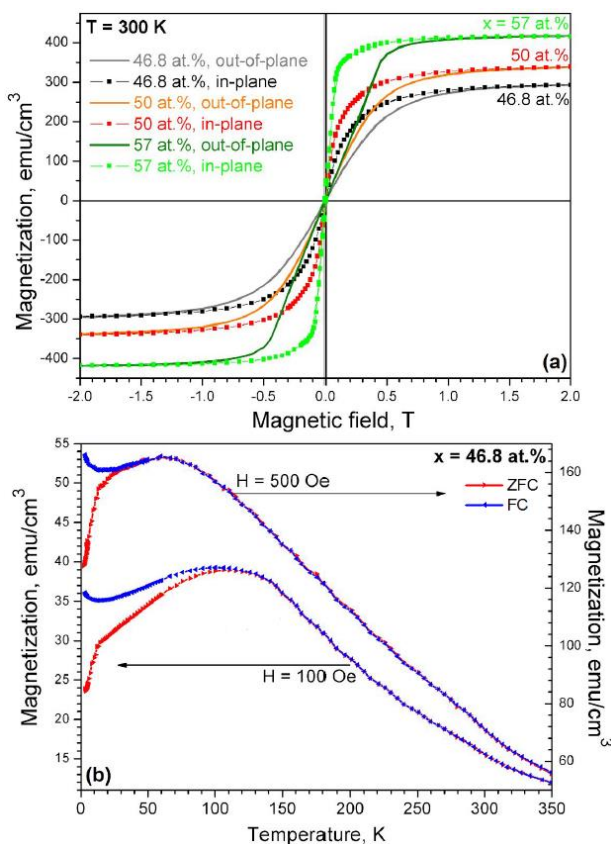


**Fig. 1.** (a) Magnetic field dependences of magnetization of samples with  $x = 46.8$  at.%, 50 at.%, and 57 at.% at room temperature. The dash-dot lines present the in-plane curves and solid lines denote out-of-plane curves. (b) Magnetization temperature dependences of sample with  $x = 46.8$  at.% measured in  $H = 100$  Oe and 500 Oe. The red curves are zero-field magnetizations (ZFC) and blue curves are field-cooled magnetizations (FC).

### 3.2. Resistivity

Fig. 2 shows that resistivity of the sample with  $x = 46.8$  at. % is at least one order of magnitude larger than for  $x = 57$  at.%. It confirms that the considered

samples composition is close to the percolation threshold. The temperature dependence of resistivity of the sample with  $x = 46.8$  at.% follows quite well the  $T^{1/2}$  law but it is not the case for samples with  $x = 57$  at.% (Fig.2). For the sample with  $x = 57$  at.% the temperature dependence of conductivity follows the  $\ln T$  behavior that accordingly to the theory of Efetov et al. [6,7] matches a strong tunnel coupling between nanogranules. Therefore the main transport mechanism in the studied compositions falls into the transition region between strong and weak tunnel coupling.

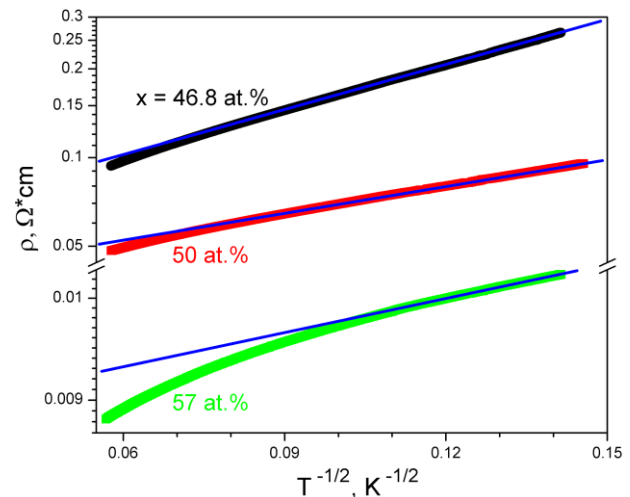


**Fig. 2.** Temperature dependences of resistivity of samples with  $x = 46.8$  at.%, 50 at.%, and 57 at.% plotted as  $\ln(\rho)$  versus  $T^{-1/2}$ .

### 3.3. Magnetoresistance

#### 3.3.1. Negative magnetoresistance

For all samples MR is small and negative in weak magnetic fields (Figs. 3-5). Negative MR can be connected with spin-dependent tunnelling, suppression of spin disorder inside ferromagnetic granules and spontaneous anisotropy (see [8]). It is quite reasonable for nanocomposites to neglect two last mechanisms. Indeed, since in studied samples granules are small the second mechanism unlikely contributes to MR. Negative MR in our case is approximately the same for magnetic field applied parallel and perpendicular to the current direction and this observation allows to completely exclude anisotropic MR. Therefore we can conclude that negative MR in the samples under investigation is due to tunneling.

Let us now discuss why tunnel MR is small, less than 1% (in comparison with record values about 10-13% at low temperatures [9,10]), and almost negligible for the sample with  $x = 57$  at. %. There are several factors which can diminish or even suppress tunnel MR: not optimal composition, wide size distribution of granules, spin-flip processes, weak spin polarization of current carriers, rough interfaces of granular surfaces, scattering by impurities or metallic atoms located inside

tunnel barriers. We think that in our case all these factors play role but the most important is the presence of a large amount of metallic atoms in the Al-O. The composition of the sample with  $x=57$  at.% is quite far from the percolation threshold and that is the reason for its extremely small negative MR.

Tunnel MR weakly depends on temperature in the Inoue-Maekawa model [11] and shows the distinctive  $1/T$  decay of the Helman-Abeles model [12]. Fig. 5 demonstrates that our data follows qualitatively the Inoue-Maekawa model, but MR decreases in the temperature range 200-300 K stronger than magnetization. Perhaps, it is connected with low tunnel barrier height in our case [3].

### 3.3.2. Positive magnetoresistance

MR reaches its greatest negative value in magnetic fields about 1- 3 T (Figs. 3 and 4) and after that instead of saturation starts to increase with magnetic field (Figs. 3 and 5). It is clearly indicate on the positive contribution to MR in high magnetic fields. Positive MR can be due to Lorentz force, MR in hopping regime, or the influence of magnetic field on e-e contribution to MR [13].

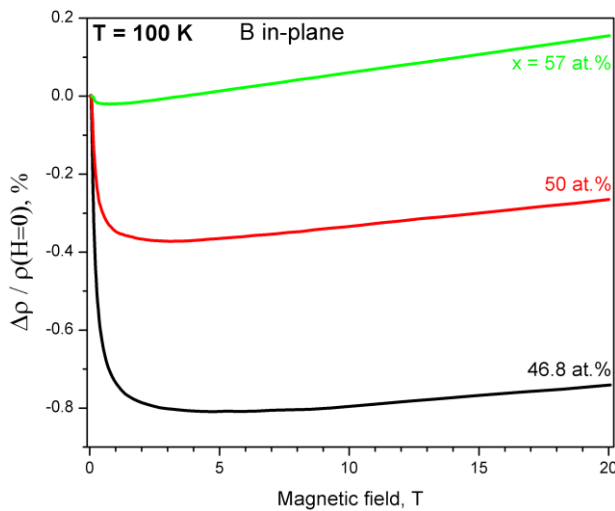


**Fig. 3.** Magnetoresistance of samples with  $x = 46.8$  at.%, 50 at.%, and 57 at.% at temperature of 100 K. The measurements were carried out with magnetic field applied parallel to the sample plane along the current.

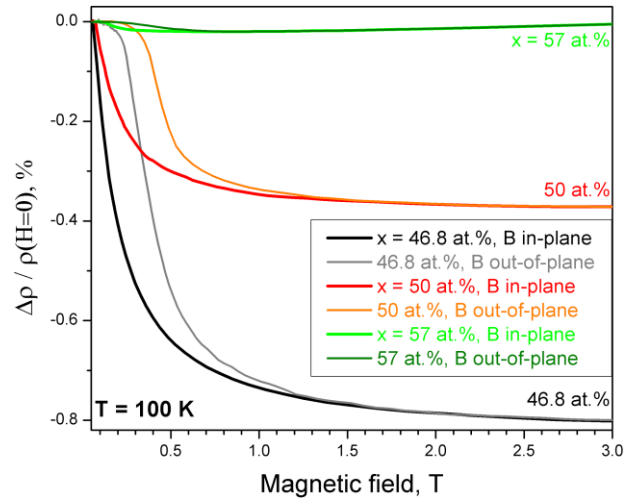


**Fig. 4.** The low magnetic field part of the magnetoresistance of samples with  $x = 46.8$  at.%, 50 at.%, and 57 at.% at temperature of 100 K for both orientations of magnetic field: in-plane and out-of-plane.

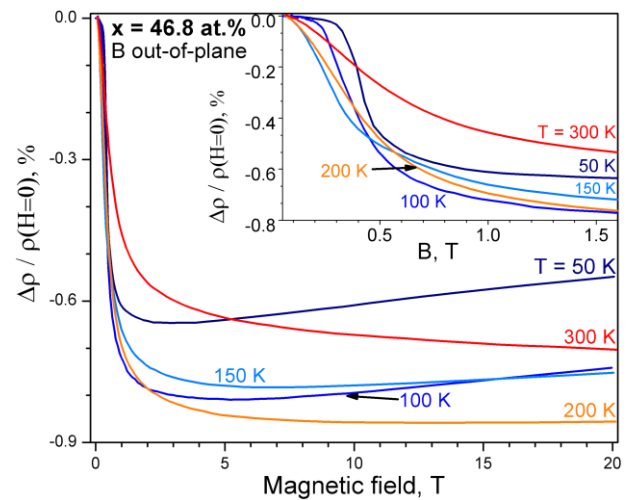


**Fig. 5.** The out-of-plane magnetoresistance of the sample with  $x = 46.8$  at.% at various temperatures  $T = 50, 100, 150, 200,$  and  $300$  K. Inset shows the low magnetic field part of the main plot.

The Lorentz MR is described by the well-known relation  $\frac{\Delta\rho}{\rho} = \frac{1}{24ne^2} \left(\frac{B}{\rho}\right)^2$ , i.e. depends quadratically on the magnetic field and is inversely proportional to the square of resistivity. However, it is not the case for our samples (Fig. 4). The positive contribution is approximately the same for samples with quite different resistivity and does not follow  $B^2$  law.

The influence of magnetic field on resistivity in hopping regime can be represented by the general form  $\rho(B)=\rho(B=0)\exp(\text{Const}B^m)$ , where  $m$  varies between 0.5 and 2 depending on the model. Our data do not correspond to this field relation. In spite of significantly different resistivity of samples with  $x=46.8$  and 57 at. %, the positive contribution to MR is almost the same. Therefore in spite of a large amount of metallic atoms in

the matrix there is no evidence of hopping transport both in resistivity and MR. The positive MR in high magnetic fields in thin films and nanogranular alloys was observed in [13] and was explained by the influence of magnetic field on e-e contribution to MR. By contrast to [13] in our case the positive MR slightly depends on resistivity and temperature. There is no evidence of significant e-e contribution to resistivity and MR.

Since the basic transport mechanism in the samples under investigations is tunneling we can suppose that the observed positive contribution to MR in high magnetic field is due to influence of magnetic field on tunnel barrier height. This hypothesis requires further experimental and theoretical researches.

This work was financially supported by the Russian Science Foundation, Grant No. 16-19-10233.

## References

1. J. J. Yang, D. B. Strukov, and D.R.Stewart, *Nat. Nanotechnol.* **8**,13 (2013)
2. M. Prezioso, F. Merrikh-Bayat, B. D. Hoskins, G.C. Adam, K. K. Likharev, D.B.Strukov, *Nature* 521, **61** (2015)
3. V. V. Rylkov, S. N. Nikolaev, K.Yu.Chernoglazov, V. A. Demin, A.V.Sitnikov, M.Yu. Presnyakov, A.L.Vasiliev, N.S. Perov, A. S. Vedeneev, Yu. E. Kalinin, V.V. Tugushev, A. B. Granovsky, *Phys. Rev. B* **95**, 144202 (2017)
4. Yu. O. Mikhailovskii, V. N. Prudnikov, V.V.Ryl'kov, K. Yu. Chernoglazov, A.V.Sitnikov, Yu. E. Kalinin, and A.B.Granovskii, *Physics of the Solid State* **58**, 444 (2016)
5. Yu. E. Kalinin, A. N. Remizov, A.V. Sitnikov, *Physics of the Solid State* **46**, 2146 (2004)
6. K. B. Efetov and A. Tschersich, *Phys. Rev. B* **67**, 174205 (2003).
7. I. S. Beloborodov, A. V. Lopatin, V.M.Vinokur, and K.B. Efetov, *Rev. Mod. Phys.* **79**, 469 (2007).
8. A. Milner, A Gerber, B. Groisman, M. Karpovsky, and A. Gladkikh, *Phys. Rev. Lett.* **76**,475 (1996)
9. Y.A. Vovk, V.O. Golub, L. Malkinski, A.F.Kravetz, A.M. Pogorely, and O.V. Shypil, *JMMM* **272-276**, e1403 (2004).
10. N. Kobayashi, S. Ohnuma, T. Masumoto, and H. Fujimori, *J. of Appl. Phys.*, **90**, 4159 (2001)
11. J. Inoue and S. Maekawa, *Phys. Rev. B* **53**, R11927 (1996).
12. J. S. Helman and B. Abeles, *Phys. Rev. Lett.* **37**, 1429 (1976).
13. A. Gerber, I. Kishon, I. Ya. Korenblit, O. Riss, A. Segal, and M. Karpovski, *Phys. Rev. Lett.* **99**, 027201 (2007)